

Study of $B_{s,d} \rightarrow l^+ l^- \gamma$ Decays

C. Q. Geng^a, C. C. Lih^a and Wei-Min Zhang^b

^a*Department of Physics, National Tsing Hua University
Hsinchu, Taiwan, Republic of China*

and

^b*Department of Physics, National Cheng Kung University
Tainan, Taiwan, Republic of China*

Abstract

We study the decays of $B_{s,d} \rightarrow l^+ l^- \gamma$ ($l = e, \mu, \tau$) within the light-front model. We calculate the tensor type form factors and use these form factors to evaluate the decay branching ratios. We find that, in the standard model, the branching ratios of $B_{s(d)} \rightarrow l^+ l^- \gamma$ ($l = e, \mu, \tau$) are 7.1×10^{-9} (1.5×10^{-10}), 8.3×10^{-9} (1.8×10^{-10}), 1.6×10^{-8} (6.2×10^{-10}), respectively.

1 Introduction

It is well known that B physics is important to determine the elements of the Cabibbo-Kobayashi-Maskawa (CKM) matrix[1] and physics beyond the standard model. Recently, the interest has been focused on the rare B meson decays induced by the flavor changing neutral current (FCNC) due to the CLEO measurement of the radiative $b \rightarrow s\gamma$ decay [2]. In the standard model, these rare decays occur at loop level and provide us information on the parameters of the CKM matrix elements as well as various hadronic form factors, such as the B meson decay constant f_B .

As in the decays of $B^+ \rightarrow l^+\nu_l$, the helicity suppression effect is also expected in the flavor changing neutral current processes of $B_{s,d} \rightarrow l^+l^-$. These decays are sensitive probes of top quark couplings [3] such as the CKM elements $V_{ts(d)}$. The decay widths of these leptonic decay modes are given by:

$$\Gamma(B_q \rightarrow l^+l^-) = \frac{\alpha^2 G_F^2 f_{B_q}^2}{16\pi^3} m_{B_q}^3 \left(\frac{m_l^2}{m_{B_q}^2} \right) |V_{tb}V_{tq}^*|^2 C_{10}^2, \quad (1)$$

where G_F is the fermi constant, M_{B_q} and m_l are B_q meson and lepton masses and C_{10} is the Wilson coefficient. Form Eq.(1), one has that $B(B_s \rightarrow e^+e^-, \mu^+\mu^-, \tau^+\tau^-) \simeq (6 \times 10^{-8}, 2.6 \times 10^{-1}, 1.0) \times 10^{-6}$ and $B(B_d \rightarrow e^+e^-, \mu^+\mu^-, \tau^+\tau^-) \simeq (4.2 \times 10^{-7}, 1.8 \times 10^{-2}, 4.5) \times 10^{-8}$ by taking $|V_{tb}V_{ts}^*| = 0.04$, $|V_{tb}V_{td}^*| = 0.01$, $f_{B_{s,d}} \simeq 200 \text{ MeV}$, $\tau_{B_s} \simeq 1.61 \text{ ps}$ and $\tau_{B_d} \simeq 1.5 \text{ ps}$ [4]. It is clear that the rates for the light lepton modes are too small to be measured due to the helicity suppressions, while that for the τ channel, although there is no suppression, it is hard to be observed experimentally because of the low efficiency.

It has been pointed out that the radiative leptonic B decays of $B^+ \rightarrow l^+\nu_l\gamma$ ($l = e, \mu$) have larger decay rates than that purely leptonic ones [5, 6, 7, 8, 9, 10, 11, 12]. Similar enhancements were also found for the radiative decays of $B_{s,d} \rightarrow l^+l^-\gamma$ in the constituent and light-cone sum rule quark models [13, 14]. In fact, the decay amplitudes of $B_{s,d} \rightarrow l^+l^-\gamma$ can be divided into the “internal-bremsstrahlung” (IB) parts, where the photon emits from the external charged leptons, which are still helicity suppressed for the light charged lepton modes, and the “structure-dependent” (SD) ones, in which one of the photon comes from intermediate states of $B_q \rightarrow l^+l^-$, which are free of the helicity suppression. Therefore, the decay rates of $B_q \rightarrow l^+l^-\gamma$ ($l = e, \mu$) might have an enhancement with respect to the purely leptonic modes of $B_q \rightarrow l^+l^-$ if the SD contributions to the decays are dominant.

In this paper, we will use the light front quark model [10, 11, 15, 16, 17, 18] to evaluate the hadronic matrix elements and study the decay rates for $B_{s,d} \rightarrow l^+ l^- \gamma$. It is known that as the recoil momentum increases, we have to start considering relativistic effects seriously. The light front quark model [18] is the widely accepted relativistic quark model in which a consistent and relativistic treatment of quark spins and the center-of-mass motion can be carried out. In this work, we calculate for the first time the tensor form factors in $P \rightarrow \gamma$ (P is a pseudoscalar meson) directly at time-like momentum transfers by using the relativistic light-front hadronic wave function. Within the framework of light-front quark model, one can calculate in the frame where the momentum transfer is purely longitudinal, *i.e.*, $p_\perp = 0$ and $p^2 = p^+ p^-$, which covers the entire range. Thus, we give their dependence on the momentum transfer p^2 in whole kinematic region of $0 \leq p^2 \leq p_{\max}^2$.

The paper is organized as follows. In Sec. 2, we present the decay amplitudes of $B_{s,d} \rightarrow l^+ l^- \gamma$. We study the form factors in the $B \rightarrow \gamma$ transition within the light front framework in Sec. 3. In Sec. 4, we calculate the decay branching ratios. We also compare our results with those in literature [13, 14, 19]. We give our conclusions in Sec. 5.

2 Decay Amplitudes

The main contributions for the processes of $B_q \rightarrow l^+ l^- \gamma$ ($l = e, \mu, \tau$) arise from the effective Hamiltonian that induces the purely leptonic modes of $B_q \rightarrow l^+ l^-$. The QCD-corrected amplitude for $b \rightarrow l^+ l^- q$ in the SM is given by [20, 21]:

$$\begin{aligned} \mathcal{M} = & -\frac{G_F \alpha}{\sqrt{2}\pi} V_{tb} V_{tq}^* \left\{ C_9^{eff} (\bar{q} \gamma_\mu P_L b) \bar{l} \gamma^\mu l + C_{10} \bar{q} \gamma_\mu P_L b \bar{l} \gamma^\mu \gamma_5 l \right. \\ & \left. - 2 \frac{C_7}{p^2} \bar{q} i \sigma_{\mu\nu} p^\nu (m_b P_R + m_q P_L) b \bar{l} \gamma^\mu l \right\}, \end{aligned} \quad (2)$$

where $q = d$ or s , $P_{L,R} = (1 \mp \gamma_5)/2$, and p is the momentum transfer, which is equal to the momentum of the lepton pair. The Wilson coefficients of C_7 , C_9^{eff} and C_{10} can be found, for example, in [20, 21, 22, 23], respectively.

The amplitude for $B_q \rightarrow l^+ l^- \gamma$ can be written as:

$$\mathcal{M}(B_q \rightarrow l^+ l^- \gamma) = \mathcal{M}_{IB} + \mathcal{M}_{SD} \quad (3)$$

where \mathcal{M}_{IB} and \mathcal{M}_{SD} represent the IB and SD contributions, respectively. For the IB part, the amplitude is clearly proportional to the lepton mass m_l and it is found to be

$$\mathcal{M}_{IB} = -ie \frac{G_F \alpha}{\sqrt{2}\pi} V_{tb} V_{tq}^* f_{B_q} C_{10} m_l \left[\bar{l} \left(\frac{\not{p}_B}{2p_1 \cdot q_\gamma} - \frac{\not{p}_B \not{q}_\gamma}{2p_2 \cdot q_\gamma} \right) \gamma_5 l \right], \quad (4)$$

where P_B , p_1 , p_2 and q_γ , are the momentum of B_q , l^+ , l^- and γ , respectively. In Eq.(4), the f_{B_q} is the B_q meson decay constant, defined by:

$$\langle 0 | \bar{s} \gamma^\mu \gamma_5 b | B_q(p) \rangle = -i f_{B_q} p^\mu. \quad (5)$$

When a photon emitted from the charged internal line, the amplitude is suppressed by a factor m_b^2/m_W^2 in the Wilson coefficients and the main contribution comes from the photon radiating from the initial quark line. Therefore \mathcal{M}_{SD} can be written as

$$\begin{aligned} \mathcal{M}_{SD} = & -\frac{G_F \alpha}{\sqrt{2}\pi} V_{tb} V_{tq}^* \left\{ C_9^{eff} \langle \gamma(q_\gamma) | \bar{q} \gamma_\mu P_L b | B(p+q_\gamma) \rangle \bar{l} \gamma^\mu l \right. \\ & + C_{10} \langle \gamma(q_\gamma) | \bar{q} \gamma_\mu P_L b | B(p+q_\gamma) \rangle \bar{l} \gamma^\mu \gamma_5 l \\ & \left. - 2 \frac{C_7 m_b}{p^2} \langle \gamma(q_\gamma) | \bar{q} i \sigma_{\mu\nu} p^\nu P_R b | B(p+q_\gamma) \rangle \bar{l} \gamma^\mu l \right\}. \end{aligned} \quad (6)$$

From the amplitude in Eq.(6), we see that to find the decay rates, one has to evaluate the hadronic matrix elements. These elements can be parameterized as follows:

$$\begin{aligned} \langle \gamma(q_\gamma) | \bar{q} \gamma_\mu \gamma_5 b | B_q(p+q_\gamma) \rangle &= -e \frac{F_{VA}}{M_{B_q}} \left[(p \cdot q_\gamma) \epsilon_\mu^* - (\epsilon^* \cdot p) q_{\gamma\mu} \right], \\ \langle \gamma(q_\gamma) | \bar{q} \gamma_\mu b | B_q(p+q_\gamma) \rangle &= ie \frac{F_{VV}}{M_{B_q}} \varepsilon_{\mu\alpha\beta\nu} \epsilon^{*\alpha} p^\beta q_\gamma^\nu, \end{aligned} \quad (7)$$

$$\begin{aligned} \langle \gamma(q_\gamma) | \bar{q} i \sigma_{\mu\nu} p^\nu \gamma_5 b | B_q(p+q_\gamma) \rangle &= ie F_{TA} \left[(p \cdot q_\gamma) \epsilon_\mu^* - (\epsilon^* \cdot p) q_{\gamma\mu} \right], \\ \langle \gamma(q_\gamma) | \bar{q} i \sigma_{\mu\nu} p^\nu b | B_q(p+q_\gamma) \rangle &= e F_{TV} \varepsilon_{\mu\nu\alpha\beta} \epsilon^{*\nu} q_\gamma^\alpha p^\beta, \end{aligned} \quad (8)$$

where the ϵ_μ is the photon polarization vector, q_γ and $p+q_\gamma$ are the four momenta of the photon and the B_q meson, and F_{VA} , F_{VV} , F_{TA} and F_{TV} are the form factors of axial-vector, vector, axial-tensor and tensor, respectively. Form Eqs.(7) and (8), we rewrite the amplitude of Eq.(6) as,

$$\begin{aligned} \mathcal{M}_{SD} = & \frac{\alpha G_F}{2\sqrt{2}\pi} V_{tb} V_{ts}^* \left\{ \varepsilon_{\mu\nu\alpha\beta} \epsilon^{*\nu} p^\alpha q_\gamma^\beta \left[A \bar{l} \gamma^\mu l + C \bar{l} \gamma^\mu \gamma_5 l \right] \right. \\ & \left. + i \left[(p \cdot q_\gamma) \epsilon_\mu^* - (\epsilon^* \cdot p) q_{\gamma\mu} \right] \left[B \bar{l} \gamma^\mu l + D \bar{l} \gamma^\mu \gamma_5 l \right] \right\}, \end{aligned} \quad (9)$$

where the factors of A - D are defined by

$$\begin{aligned} A &= \frac{C_9^{eff}}{M_B} F_{VA}(p^2) - 2 C_7 \frac{m_b}{p^2} F_{TA}(p^2), \\ B &= \frac{C_9^{eff}}{M_B} F_{VV}(p^2) - 2 C_7 \frac{m_b}{p^2} F_{TV}(p^2), \\ C &= \frac{C_{10}}{M_B} F_{VA}(p^2), \\ D &= \frac{C_{10}}{M_B} F_{VV}(p^2), \end{aligned} \quad (10)$$

respectively. The form factors of F_{VA} and F_{VV} have been evaluated previously in the light-front model [10], while that of F_{TA} and F_{TV} shall be studied in the next section.

3 Form Factors in the Light Front Model

In this section, we will use the light-front approach to calculate the tensor type form factors in Eq. (8) for $B_q \rightarrow \gamma$ ($q = s$ or d) transition. In this approach, the B meson bound state consists of an anti-quark \bar{b} and a quark q with the total momentum of $(p + q_\gamma)$ and it is given by

$$|B(p + q_\gamma) > = \sum_{\lambda_1 \lambda_2} \int [dk_1][dk_2] 2(2\pi)^3 \delta^3(p + q_\gamma - k_1 - k_2) \\ \times \Phi_B^{\lambda_1 \lambda_2}(x, k_\perp) b_b^+(k_1, \lambda_1) d_q^+(k_2, \lambda_2) |0 >, \quad (11)$$

where $k_{1(2)}$ is the on-mass shell light front momentum of the internal quark $\bar{b}(q)$, the light front relative momentum variables (x, k_\perp) are defined by

$$k_1^+ = x(p + q_\gamma)^+, \quad k_{1\perp} = x(p + q_\gamma)_\perp + k_\perp, \quad (12)$$

and

$$\Phi_B^{\lambda_1 \lambda_2}(x, k_\perp) = \left(\frac{2k_1^+ k_2^+}{M_0^2 - (m_q - m_b)^2} \right)^{\frac{1}{2}} \bar{u}(k_1, \lambda_1) \gamma^5 v(k_2, \lambda_2) \phi(x, k_\perp), \quad (13)$$

with $\phi(x, k_\perp)$ being the momentum distribution amplitude. The amplitude of $\phi(x, k_\perp)$ can be solved in principle by the light-front QCD bound state equation[24, 25]. Here, we use the Gaussian type wave function:

$$\phi(x, k_\perp) = N \sqrt{\frac{dk_z}{dx}} \exp \left(-\frac{\vec{k}_\perp^2}{2\omega_B^2} \right), \quad (14)$$

where

$$[dk_1] = \frac{dk^+ dk_\perp}{2(2\pi)^3}, \quad N = 4 \left(\frac{\pi}{\omega_B^2} \right)^{\frac{3}{4}}, \\ k_z = \left(x - \frac{1}{2} \right) M_0 + \frac{m_b^2 - m_q^2}{2M_0}, \quad M_0^2 = \frac{k_\perp^2 + m_q^2}{x} + \frac{k_\perp^2 + m_b^2}{1-x}, \\ \sum_\lambda u(k, \lambda) \bar{u}(k, \lambda) = \frac{m + \not{k}}{k^+}, \quad \sum_\lambda v(k, \lambda) \bar{v}(k, \lambda) = -\frac{m - \not{k}}{k^+}. \quad (15)$$

We note that the wave function in Eq.(14) could be also applied to many other of hadronic transitions. For the gauged photon state, one has [10]

$$|\gamma(q_\gamma) > = N' \left\{ a^+(q_\gamma, \lambda) + \sum_{\lambda_1 \lambda_2} \int [dk_1][dk_2] 2(2\pi)^3 \delta^3(q_\gamma - k_1 - k_2) \right. \\ \left. \times \Phi_{q\bar{q}}^{\lambda_1 \lambda_2 \lambda}(q_\gamma, k_1, k_2) b_q^+(k_1, \lambda_1) d_{\bar{q}}^+(k_1, \lambda_2) \right\} |0 >, \quad (16)$$

where

$$\Phi_{q\bar{q}}^{\lambda_3 \lambda_4 \lambda}(q_\gamma, k_1, k_2) = \frac{e_q}{ED} \chi_{-\lambda_2}^+ \left\{ -2 \frac{q_{\gamma\perp} \cdot \epsilon_\perp}{q_\gamma^+} - \tilde{\sigma}_\perp \cdot \epsilon_\perp \frac{\tilde{\sigma}_\perp \cdot k_{2\perp} + im_2}{k_2^+} \right. \\ \left. - \frac{\tilde{\sigma}_\perp \cdot k_{1\perp} + im_1}{k_1^+} \tilde{\sigma}_\perp \cdot \epsilon_\perp \right\} \chi_{\lambda_1}, \quad (17)$$

with

$$ED = \frac{q_{\gamma\perp}^2}{q_\gamma^+} - \frac{k_{1\perp}^2 + m_1^2}{k_1^+} - \frac{k_{2\perp}^2 + m_2^2}{k_2^+}. \quad (18)$$

In Eq. (17), we have used the two-component form of the light-front quark fields [26, 18]. Since the physically accessible kinematic region is $0 \leq p^2 \leq p_{\max}^2$ where $p_{\max}^2 = M_B^2$, to calculate the matrix elements in Eq. (8), we choose a frame where the transverse momentum $p_\perp = 0$. Then $p^2 = p^+ p^- \geq 0$ which can cover the entire range of the momentum transfers. By considering the “good” component of $\mu = +$, the tensor current in Eq. (8) can be rewritten as:

$$< \gamma(q_\gamma) | (q_+^+ \gamma^0 \gamma_5 b_- - q_-^+ \gamma^0 \gamma_5 b_+) | B(p + q_\gamma) > = e F_{TA} (\epsilon_\perp^* \cdot q_{\gamma\perp}), \\ < \gamma(q_\gamma) | (q_+^+ \gamma^0 b_- - q_-^+ \gamma^0 b_+) | B(p + q_\gamma) > = -ie F_{TV} \epsilon^{ij} \epsilon_i^* q_{\gamma j}, \quad (19)$$

where $q_+(b_+)$ and $q_-(b_-)$ are the light-front up and down component of the quark fields. In the two-component form [26, 18], they are expressed by

$$q_+ = \begin{pmatrix} \chi \\ 0 \end{pmatrix} \quad (20)$$

and

$$q_- = \frac{1}{i\partial^+} (i\alpha_\perp \cdot \partial_\perp + \beta m_q) q_+ = \begin{pmatrix} 0 \\ \frac{1}{\partial^+} (\tilde{\sigma}_\perp \cdot \partial_\perp + m_q) \chi_q \end{pmatrix}. \quad (21)$$

In Eq. (21), χ_q is a two-component spinor field and σ is the Pauli matrix. The form factors of F_{TA} and F_{TV} in Eqs. (19) are then found to be:

$$F_{TA}(p^2) = \int \frac{dx d^2 k_\perp}{2(2\pi)^3} \Phi(x', k_\perp^2) \\ \times \left\{ \frac{1}{3} \frac{A_1 + A_2 k_\perp^2 \Theta}{m_b^2 + k_\perp^2} + \frac{1}{3} \frac{B_1 + B_2 k_\perp^2 \Theta}{m_q^2 + k_\perp^2} \right\} \quad (22)$$

and

$$F_{TV}(p^2) = - \int \frac{dx d^2 k_\perp}{2 (2\pi)^3} \Phi(x', k_\perp^2) \times \left\{ \frac{1}{3} \frac{C_1 + C_2 k_\perp^2 \Theta}{m_b^2 + k_\perp^2} + \frac{1}{3} \frac{D_1 + D_2 k_\perp^2 \Theta}{m_q^2 + k_\perp^2} \right\} \quad (23)$$

where

$$\begin{aligned} A_1 &= \frac{2}{xx'^2(1-x')(1-x)} \left\{ (x' + x - 2x'x) [x'(x-1) - x(2x-1)] k_\perp^2 \right. \\ &\quad \left. + x [(x-x') + 2x'x(1-x)] m_b^2 + 2x^2(1-x')^2 m_b m_q \right\}, \\ A_2 &= \frac{2(x-x')}{xx'^2(1-x')(1-x)} \left\{ (x' + x - 2x'x)(1-2x) k_\perp^2 \right. \\ &\quad \left. + 2x(1-x') m_q m_b - x(1-2x)(1-x')^2 m_q^2 + x'(1+x'x - 2xx'^2) m_b^2 \right\}, \\ B_1 &= \frac{2}{x'x(1-x)(1-x')^2} \left\{ (x' + x - 2x'x)(1-2x + 2x^2 - x'x) k_\perp^2 \right. \\ &\quad \left. + 2xx'(1-x')(1-x) m_q m_b + (1-x')(x' + x - 4x'x + 2x'x^2) m_q^2 \right\}, \\ B_2 &= \frac{2(x-x')}{x'x(1-x)(1-x')^2} \left\{ -(x' + x - 2x'x)(1-2x) k_\perp^2 \right. \\ &\quad \left. - [(1-2x)x'^2(1-x) m_b^2 + (1-x')(x' + x - 3x'x - 2x^2(1-x')) m_q^2] \right\}, \\ C_1 &= \frac{2}{xx'^2(1-x')(1-x)} \left\{ (x - x' + xx')(x' + x - 2x'x) k_\perp^2 \right. \\ &\quad \left. - 2x^2(1-x')^2 m_b m_q + x' [(x-x') - 2(1-x')x^2] m_b^2 \right\}, \\ C_2 &= \frac{2(x-x')}{xx'^2(1-x')(1-x)} \left\{ (x' + x - 2x'x) k_\perp^2 + x'(1-2x + xx') m_b^2 \right. \\ &\quad \left. - m_q^2 x(1-x')^2 - 2x(1-x') m_q m_b \right\}, \\ D_1 &= \frac{2}{x(1-x)x'(1-x')^2} \left\{ -(1-x)(1-2x+x')(x' + x - 2x'x) k_\perp^2 \right. \\ &\quad \left. - [(1-x')(x' + x - 2x^2 - 2x'x + 2x^2 x') m_q^2 + 2x'^2(1-x)^2 m_q m_b] \right\}, \\ D_2 &= \frac{2(x-x')}{x'(1-x)x(1-x')^2} \left\{ (x' + x - 2x'x) k_\perp^2 + x'^2(1-x) m_b^2 \right. \\ &\quad \left. + (1-x')(x' - x - x'x) m_q^2 \right\}, \\ \Phi(x, k_\perp^2) &= N \left(\frac{2x(1-x)}{M_0^2 - (m_q - m_b)^2} \right)^{1/2} \sqrt{\frac{dk_z}{dx}} \exp \left(-\frac{\vec{k}^2}{2\omega_B^2} \right), \end{aligned}$$

$$\begin{aligned}\Theta &= \frac{1}{\Phi(x, k_\perp^2)} \frac{d\Phi(x, k_\perp^2)}{dk_\perp^2}, \\ x' &= x \left(1 - \frac{p^2}{M_B^2}\right), \quad \vec{k} = (\vec{k}_\perp, \vec{k}_z).\end{aligned}\tag{24}$$

To illustrate numerical results, we input $m_q = m_s = 0.4$, $m_b = 4.5$ in GeV , and $\omega = 0.55$ GeV which is determined by fitting $f_{B_s} = 200$ GeV via Eq. (5). The values of F_{TA} and F_{TV} in the entire range of p^2 are shown in Fig. 2. We note that the tails of $F_{TV,TA}$ at the large momentum transfers go down may be the long distance contribution associated with $B - B^* - \gamma$ vertex, which is not included in the present work. It is interesting to note that the formulas in Eqs. (22) and (23) can be used for other pseudoscalars, such as pions and kaons, to the photon transitions as well once we put in the corresponding masses.

4 Decay Branching Ratios

The partial decay width for $B_q \rightarrow l^+ l^- \gamma$ in the B rest frame is given by

$$d\Gamma = \frac{1}{2M_B} |\mathcal{M}|^2 (2\pi)^4 \delta^4(P_B - p_1 - p_2 - q_\gamma) \frac{d\vec{q}_\gamma}{(2\pi)^3 2E_\gamma} \frac{d\vec{p}_1}{(2\pi)^3 2E_1} \frac{d\vec{p}_2}{(2\pi)^3 2E_2},\tag{25}$$

where the square of the matrix element can be written as

$$|\mathcal{M}|^2 = |\mathcal{M}_{IB}|^2 + |\mathcal{M}_{SD}|^2 + 2Re(\mathcal{M}_{IB}\mathcal{M}_{SD}^*).\tag{26}$$

To describe the kinematic of $B_q \rightarrow l^+ l^- \gamma$, we defined two variables of $x_\gamma = 2P_B \cdot q_\gamma / M_B$ and $y = 2P_B \cdot p_1 / M_B$. One can easily write the transfer momentum p^2 in term of x_γ as

$$p^2 = M_B^2(1 - x_\gamma).\tag{27}$$

The double differential decay rate is found to be

$$\frac{d^2\Gamma^l}{dx_\gamma d\lambda} = \frac{M_B}{256\pi^3} |M|^2 = C\rho(x_\gamma, \lambda),\tag{28}$$

where

$$C = \alpha \left| \frac{\alpha V_{tb} V_{ts}^*}{8\pi^2} \right|^2 G_F^2 M_B^5,\tag{29}$$

and

$$\rho(x_\gamma, \lambda) = \rho_{IB}(x_\gamma, \lambda) + \rho_{SD}(x_\gamma, \lambda) + \rho_{IN}(x_\gamma, \lambda),\tag{30}$$

with

$$\begin{aligned}
\rho_{IB} &= 4|f_B C_{10}|^2 \frac{r_l}{M_B^2 x_\gamma^2} \left\{ \frac{x_\gamma^2 - 2x_\gamma + 2 - 4r_l}{\lambda(1-\lambda)} - 2r_l \left(\frac{1}{\lambda^2} + \frac{1}{(1-\lambda)^2} \right) \right\}, \\
\rho_{SD} &= \frac{M_B^2}{8} x_\gamma^2 \left\{ (|A|^2 + |B|^2) \left[(1 - x_\gamma + 2r_l) - 2(1 - x_\gamma)(\lambda - \lambda^2) \right] \right. \\
&\quad + (|C|^2 + |D|^2) \left[(1 - x_\gamma - 2r_l) - 2(1 - x_\gamma)(\lambda - \lambda^2) \right] \\
&\quad \left. + 2\text{Re}(B^*C + A^*D)(1 - x_\gamma)(2\lambda - 1) \right\}, \\
\rho_{IN} &= f_B C_{10} r_l \left\{ \text{Re}(A) \frac{x_\gamma}{\lambda(1-\lambda)} + \text{Re}(D) \frac{x_\gamma(1-2\lambda)}{\lambda(1-\lambda)} \right\}. \tag{31}
\end{aligned}$$

Here $\lambda = (x_\gamma + y - 1)/x_\gamma$ and $r_l = m_l^2/M_B^2$ and the physical regions for x_γ and λ are given by:

$$\begin{aligned}
0 &\leq x_\gamma \leq 1 - 4r_l, \\
\frac{1}{2} - \frac{1}{2} \sqrt{1 - \frac{4r_l}{1-x_\gamma}} &\leq \lambda \leq \frac{1}{2} + \frac{1}{2} \sqrt{1 - \frac{4r_l}{1-x_\gamma}}. \tag{32}
\end{aligned}$$

For the Wilson coefficients C_7 and C_{10} , we use the results given by Refs.[20, 21] and they are

$$C_7 = -0.315, \quad C_{10} = -4.642.$$

The analytic expressions for C_9^{eff} in the next-to-leading order approximation is given by[23]:

$$\begin{aligned}
C_9^{eff} &= C_9 + 0.124w(s) + g(\hat{m}_c, s)(3C_1 + C_2 + 3C_3 + C_4 + 3C_5 + C_6) \\
&\quad - \frac{1}{2}g(\hat{m}_q, s)(C_3 + 3C_4) - \frac{1}{2}g(\hat{m}_b, s)(4C_3 + 4C_4 + 3C_5 + C_6) \\
&\quad + \frac{2}{9}(3C_3 + C_4 + 3C_5 + C_6), \tag{33}
\end{aligned}$$

with

$$\begin{aligned}
C_9 &= 4.227, \\
(3C_1 + C_2 + 3C_3 + C_4 + 3C_5 + C_6) &= 0.359, \\
(C_3 + 3C_4) &= -0.0659, \\
(4C_3 + 4C_4 + 3C_5 + C_6) &= -0.0675, \\
(3C_3 + C_4 + 3C_5 + C_6) &= -0.00157, \tag{34}
\end{aligned}$$

and $s = p^2/m_b^2$. In the Eq.(33), the function of $w(\hat{s})$ comes from the single-gluon correction to the matrix element of O_9 and its form can be found in Refs.[21, 22], while that of $g(\hat{m}_i, s)$ from the one loop contributions of the four quark operators $O_1 - O_6$, given by [21, 23]:

$$g(\hat{m}_i, s) = -\frac{8}{9} \ln \hat{m}_i + \frac{8}{27} + \frac{4}{9} y_i - \frac{2}{9} (2 + y_i) \sqrt{|1 - y_i|} \\ \times \begin{cases} (\ln \frac{1+\sqrt{1-y_i}}{1-\sqrt{1-y_i}} - i\pi) & \text{for } y_i < 1 \\ 2 \arctan \frac{1}{\sqrt{y_i-1}} & \text{for } y_i > 1 \end{cases} \quad (35)$$

with $y_i = \hat{m}_i^2/s$ and $\hat{m}_i = m_i/m_b$. By taking into account the long distance effects mainly due to the J/ψ family resonances, one may use the replacement[27]

$$g(\hat{m}_c, s) \rightarrow g(\hat{m}_c, s) - \frac{3\pi}{\alpha^2} \sum_{V=J/\psi, \psi'} \frac{\hat{m}_V Br(V \rightarrow l^+ l^-) \hat{\Gamma}_{tot}^V}{s - \hat{m}_V^2 + i \hat{m}_V \hat{\Gamma}_{tot}^V} \quad (36)$$

where $\hat{m}_V = m_V/m_b$ and $\hat{\Gamma}_{tot} = \Gamma/m_b$. The masses and decay widths of the corresponding mesons in Eq.(35) are listed[4] in table 1.

Table 1: Charmonium mass and width

Meson	Mass (GeV)	$Br(V \rightarrow l^+ l^-)$	$\Gamma_{total}(MeV)$
J/ψ	3.097	6.0×10^{-2}	0.088
ψ	3.686	8.3×10^{-3}	0.277

In Figs.2 and 3 we present the differential decay rates of $B_s \rightarrow \mu^+ \mu^- \gamma$ and $B_s \rightarrow \tau^+ \tau^- \gamma$ as functions of x_γ , with and without resonance (J/ψ and ψ') contributions. From these figures we see that the contributions from the IB parts, corresponding to small x_γ region, are infrared divergence. To obtain the decay width of $B_s \rightarrow \tau^+ \tau^- \gamma$, a cut on the photon energy is needed. Our results for the integrated branching ratios without and with long-distance effects as well as those given by the constituent quark model [14] and the light-cone QCD sum rule model [13, 19] are summarized in tables 2 and 3, respectively. Here, we have used the cut value of $\delta = 0.01$ and $m_c = 1.5 \text{ GeV}$, $m_s = 0.4 \text{ GeV}$, $|V_{tb} V_{ts}^*| = 0.045$, $|V_{tb} V_{td}^*| = 0.01$, $\tau(B_s) = 1.61 \times 10^{-12} \text{ s}$ and $\tau(B_d) = 1.5 \times 10^{-12} \text{ s}$ [4].

We now compare our results with those in the literature [13, 14, 19]. As shown in Table 2, the decay branching ratios for $B_s \rightarrow l^+ l^- \gamma$ ($l = e, \mu$) without long distance contributions found in our calculations are smaller than those in the constituent quark model [14], whereas for $B_d \rightarrow l^+ l^- \gamma$ the statement are much smaller than ones. It is mainly due to that in the constituent quark model [14] the decay rate of $B_q \rightarrow l^+ l^- \gamma$ is proportional to the inverse of the quark mass m_q . It is interesting to see that our

Table 2: Integrated branching ratios for the radiative leptonic $B_{s,d}$ decays without long-distance

Integrated Decay Branching Ratios	IB	SD	IN	Sum	Ref. [14]	Ref. [13, 19]
$10^9 B(B_s \rightarrow e^+ e^- \gamma)$	3.1×10^{-5}	3.2	5.2×10^{-6}	3.2	6.2	2.35
$10^9 B(B_s \rightarrow \mu^+ \mu^- \gamma)$	5.5×10^{-1}	3.2	8.2×10^{-2}	3.8	4.6	1.9
$10^9 B(B_s \rightarrow \tau^+ \tau^- \gamma)$ (Cut $\delta = 0.01$)	13.0	0.6	6.4×10^{-1}	14.2	—	9.54
$10^{10} B(B_d \rightarrow e^+ e^- \gamma)$	1.4×10^{-5}	1.5	2.4×10^{-6}	1.5	8.2	1.5
$10^{10} B(B_d \rightarrow \mu^+ \mu^- \gamma)$	2.6×10^{-1}	1.5	3.8×10^{-2}	1.8	6.2	1.2
$10^{10} B(B_d \rightarrow \tau^+ \tau^- \gamma)$ (Cut $\delta = 0.01$)	5.7	2.4×10^{-1}	2.7×10^{-1}	6.1	—	—

Table 3: Integrated branching ratios for the radiative leptonic $B_{s,d}$ decays with long-distance

Integrated Decay Branching Ratios	IB	SD	IN	Sum	Ref. [19]
$10^9 B(B_s \rightarrow e^+ e^- \gamma)$	3.1×10^{-5}	7.1	5.8×10^{-6}	7.1	—
$10^9 B(B_s \rightarrow \mu^+ \mu^- \gamma)$	5.5×10^{-1}	7.1	9.4×10^{-2}	8.3	—
$10^9 B(B_s \rightarrow \tau^+ \tau^- \gamma)$ (Cut $\delta = 0.01$)	13.0	1.9	7.9×10^{-1}	15.7	15.2
$10^{10} B(B_d \rightarrow e^+ e^- \gamma)$	1.4×10^{-5}	1.5	2.4×10^{-6}	1.5	—
$10^{10} B(B_d \rightarrow \mu^+ \mu^- \gamma)$	2.6×10^{-1}	1.5	3.8×10^{-2}	1.8	—
$10^{10} B(B_d \rightarrow \tau^+ \tau^- \gamma)$ (Cut $\delta = 0.01$)	5.7	2.3×10^{-1}	2.5×10^{-1}	6.2	—

results are close to those in the light-cone QCD sum rule model [13, 19]. We note that the SD contributions for the decays in both constituent quark and light-cone QCD sum rule models are sensitive to the values of the decay constants $f_{B_{s,d}}$.

5 Conclusions

We have studied the decays of $B_{s,d} \rightarrow l^+ l^- \gamma$ within the light-front model. We have calculated the tensor type form factors and used these form factors to evaluate the decay branching ratios. We have found that, in the standard model, the branching ratios of $B_{s(d)} \rightarrow e^+ e^- \gamma$, $B_{s(d)} \rightarrow \mu^+ \mu^- \gamma$ and $B_{s(d)} \rightarrow \tau^+ \tau^- \gamma$ are 7.1×10^{-9} (1.5×10^{-10}), 8.3×10^{-9} (1.8×10^{-10}) and 1.6×10^{-8} (6.2×10^{-10}), respectively. Comparing with the purely lep-

tonic decays of $B_{s,d} \rightarrow l^+l^-$, we have shown that the branching ratios of $B_{s,d} \rightarrow l^+l^-\gamma$ have the same order of magnitude for the μ channel but that of $B_{s,d} \rightarrow e^+e^-\gamma$ are much larger. We conclude that some of the radiative leptonic decays of $B_{s,d} \rightarrow l^+l^-\gamma$ could be measured in the B factories as well as LHC-B experiments, where approximately, $6 \times 10^{11}(2 \times 10^{11})$ $B_d(B_s)$ mesons are expected to be produced per year.

Acknowledgments

This work was supported in part by the National Science Council of the Republic of China under contract number NSC-89-2112-M-007-013 and NSC-89-2112-M-006-026 .

References

- [1] N. Cabibbo, *Phys. Rev. Lett.* **10** (1963) 531; M. Kobayashi and T. Maskawa, *Prog. Theor. Phys.* **49** (1973) 652.
- [2] CLEO Collaboration, R. Ammar et. al., *Phys. Rev. Lett.* **71** (1993) 674.
CLEO Collaboration, M. S. Alam et. al., *Phys. Rev. Lett.* **74** (1995) 2885.
- [3] B. A. Campbell and P. J. O'Donnell, *Phys. Rev.* **D25**, 1989 (1982).
- [4] Particle Data Group, *Eur. Phys. Soc. J.* **C3**, 1 (1998).
- [5] G. Burdman, T. Goldman and D. Wyler, *Phys. Rev.* **D51**, 111 (1995).
- [6] G. Eilam, I. Halperin and R. Mendel, *Phys. Lett.* **B361**, 137 (1995).
- [7] D. Atwood, G. Eilam and A. Soni *Mod. Phys. Lett.* **A11**, 1061 (1996).
- [8] P. Colangelo, F. De Fazio, G. Nardulli, *Phys. Lett.* **B372**, 331 (1996); **B386**, 328 (1996).
- [9] T. Aliev, A. Özpineci and M. Savci, *Phys. Lett.* **B393**, 143 (1997); *Phys. Rev.* **D55**, 7059 (1997).
- [10] C. Q. Geng, C. C. Lih and W. M. Zhang, *Phys. Rev.* **D57** 5697(1998).
- [11] C. C. Lih, C. Q. Geng and W. M. Zhang, *Phys. Rev.* **D59** (1999) 114002.
- [12] Gregory P. Korchemsky, Dan Pirjol and Tung-Mow Yan, *Phys.Rev.* **D61** (2000) 114510.
- [13] T. M. Aliev, A. Özpineci and M. Savci, *Phys. Rev.* **D55**, 7059 (1997).
- [14] G. Eilam, C.-D. Lü and D.-X. Zhang, *Phys. Lett.* **B391**, 461 (1997).
- [15] M. Terent'ev, *Sov. J. Phys.* **24**, 106 (1976); V. Berestetsky and M. Terent'ev, *ibid* **24**, 547 (1976); **25**, 347 (1977); P. Chung, F. Coester and W. Polyzou, *Phys. Lett.* **B205**, 545 (1988).
- [16] W. Jaus, *Phys. Rev.* **D41**, 3394 (1990); **44**, 2851 (1991); P. J. O'Donnell and Q. P. Xu, *Phys. Lett.* **B325**, 219; **336**, 113 (1994).

- [17] Hai-Yang Cheng, Chi-Yee Cheung and Chien-Wen Hwang, Phys. Rev. **D55**, 1559 (1997).
- [18] Also see a review by W. M. Zhang, Chin. J. Phys. **31**, 717 (1994).
- [19] T. M. Aliev, N. K. PAK and M. Savci, Phys.Lett. **B424** (1998) 175.
- [20] G. Buchalla, A. J. Buras and M. E. Lautenbacher, Rev.Mod.Phys.**68** (1996) 1125-1144; A. J. Buras and M. Münz, Phys. Rev. **D52** (1995) 186; B. Grinstein, M. J. Savage and M. B. Wise, Nucl. Phys. bf B319 (1989) 271.
- [21] M. Misiak, Nucl. Phys. **B393** (1993) 23; Erratum: ibid **B439** (1995) 461.
- [22] M. Misiak, Nucl. Phys. **B439** (1995) 461;
- [23] F. Krüger, L. M. Sehgal Phys. Lett **B380** (1996) 199;
- [24] K. G. Wilson, T. Walhout, A. Harindranath, W. M. Zhang, R. J. Perry and S. Glazek Phys.Rev. **D49** (1994) 6720-6766
- [25] W. M. Zhang, Phys. Rev. **D56** (1997) 1528.
- [26] W. M. Zhang and A. Harindranath, Phys. Rev. **D48** (1993) 4881.
- [27] C. S. Lim, T. Morozumi and A. I. Sanda, Phys. Lett. **B218** (1989) 343;
N. G. Deshpande, J. Trampetic and K. Panose, Phys. Rev. **D39** (1989) 1461;
P. J. O'Donnell and H. K. K. Tung, ibid **D43** (1991) R2067.

Figure Captions

- Figure 1: The values of the form factors F_{TA} (solid curve) and F_{TV} (dashed curve) as functions of the momentum transfer p^2 for $B_s \rightarrow \gamma$.
- Figure 2: The differential decay branching ratio $dB(B_s \rightarrow \mu^+ \mu^- \gamma)/dx_\gamma$ as a function of $x_\gamma = 2E_\gamma/M_{B_s}$ with (solid curve) and without (dashed curve) long distance.
- Figure 3: The differential decay branching ratio $dB(B_s \rightarrow \tau^+ \tau^- \gamma)/dx_\gamma$ as a function of $x_\gamma = 2E_\gamma/M_{B_s}$ with (solid curve) and without (dashed curve) long distance.

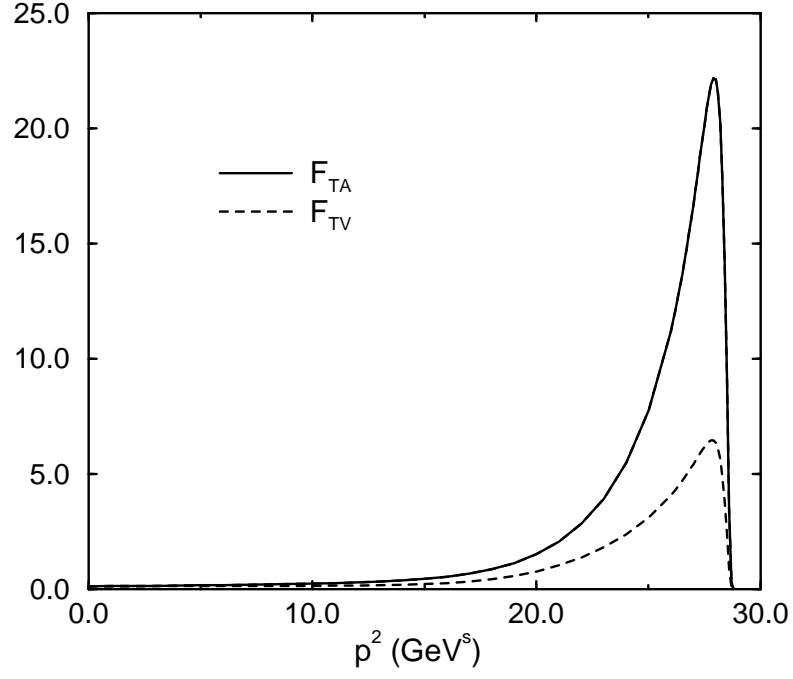


Figure 1: The values of the form factors F_{TA} (solid curve) and F_{TV} (dashed curve) as functions of the momentum transfer p^2 for $B_s \rightarrow \gamma$.

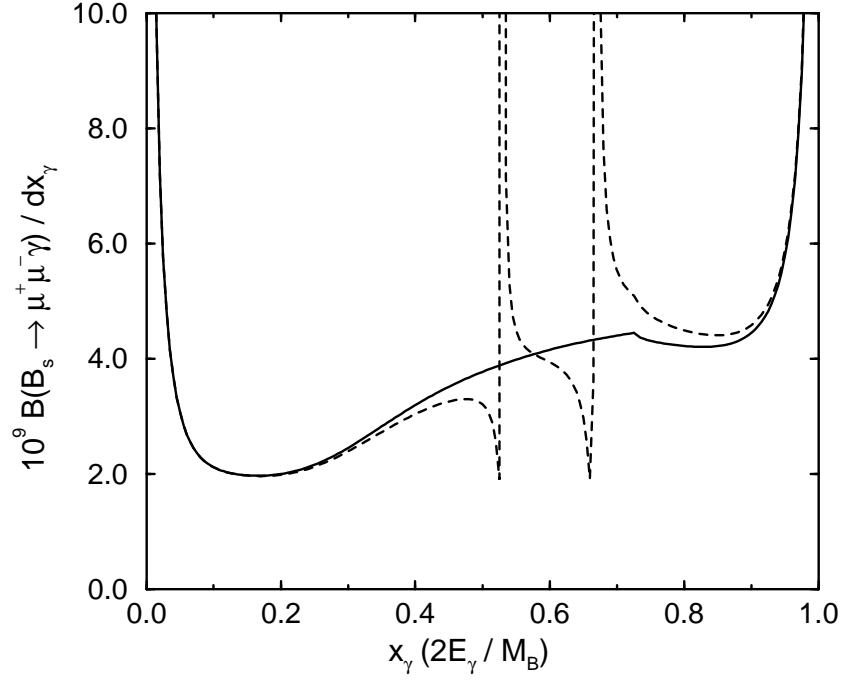


Figure 2: The differential decay branching ratio $dB(B_s \rightarrow \mu^+ \mu^- \gamma)/dx_\gamma$ as a function of $x_\gamma = 2E_\gamma/M_{B_s}$ with (solid curve) and without (dashed curve) long distance.

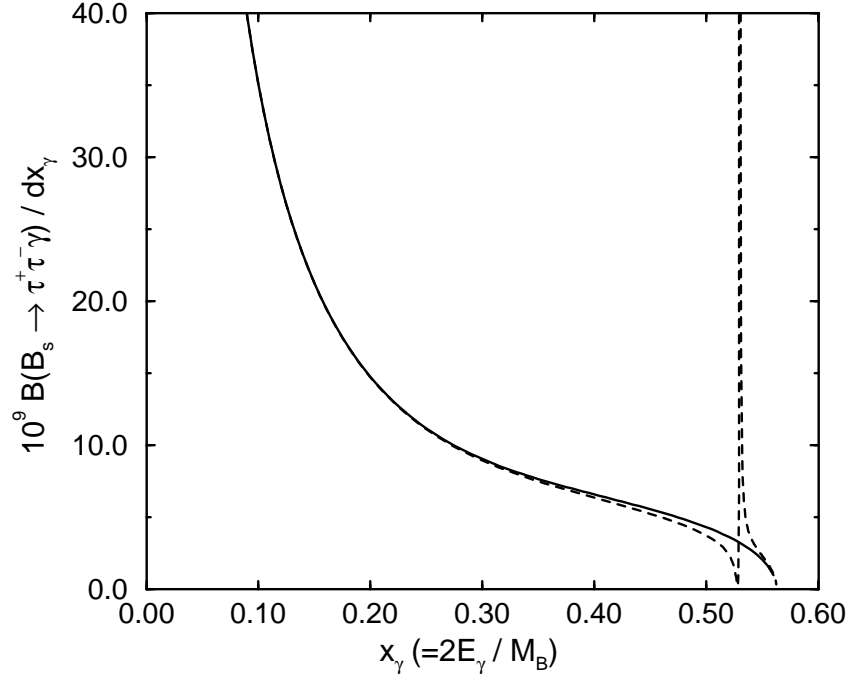


Figure 3: The differential decay branching ratio $dB(B_s \rightarrow \tau^+ \tau^- \gamma)/dx_\gamma$ as a function of $x_\gamma = 2E_\gamma/M_{B_s}$ with (solid curve) and without (dashed curve) long distance.